Journal of Harbin Engineering University
ISSN: 1006-7043
Vol 44 No. 8
August 2023

Analytic Networking Process Based on Geomantic and Remote Sensing for Land Degradation Monitoring of Mosul City

Amjed Naser Al-Hameedawi[1], Abbas Mohammed Noori[2*], Abdul Razzak T. Ziboon[3], Mohammed Sellab Hamza[3]

[1]Civil Engineering Department, University of Technology, Baghdad, Iraq
[2]Department of Surveying Engineering, Technical Engineering College of Kirkuk, Northern Technical University, Kirkuk 36001, Iraq
[3]Al-Esraa University College, Baghdad, Iraq

Abstract-Land degradation has recently emerged as a major environmental concern as a result of human activity and climate change. A wide range of land use/cover changes are taking place in many parts of Iraq. The primary causes of land degradation in the City of Mosul are rapid population growth, severe soil erosion, deforestation, insufficient vegetative cover, and uneven agriculture and livestock production. In the present work, remote sensing data, GIS tools, and Analytic Networking Process (ANP) were conducted for modeling land degradation. Landsat images were used for two periods, namely period between 2013 and 2021. However, Maximum Likelihood classification (ML) was used to classify images. The overall accuracy of post-classification images in different satellite data in 2013 and 2021 were 97.55 %, 98.91%, with kappa coefficients, 0.9627, and 0.9840 respectively. The finding revealed that the extremely degraded area was 64.546200 km^2 which is changing of land cover from vegetation to urban. This is while the very raw degraded area was 167.342400 km^2 which is changing of land cover from soil to bare soil. Areas of degradation of extreme regions that have been transformed from vegetation class to urban and bare soil classes, as well as those that have changed from soil class to urban and bare soil classes, are considered the most degraded areas.

Keywords: ANP, Multicriteria, ML classification, Geomantic, GIS, Land degradation

1. Introduction

Environmental deterioration has occurred over the last few decades, which includes both climate-related changes and human-induced adjustments, such as overgrazing which causes damage to grassland and agriculture (Collado et al., 2002). The occurrence of deterioration disturbs food security, local economic growth and conservation measures for natural resources, hence a repeatable and spatially explicit measurement is urgently required (S. Chen and Rao, 2008). Arable farmland is deteriorating at an alarming rate in dry regions, putting millions of producers' resources at risk (Shareef and Hasan, 2019). Satellite remote sensing can play an important part in delivering information on local, regional, and global scales on land cover and land use and land cover alteration (Jayanth et al., 2022).

Arid and semi-arid ecosystems have been effectively monitored using optical remote sensing data to identify degradation features and track inclinations of land degradation, land cover, and changes of lands (Geerken and Ilaiwi, 2004). By observing an object or phenomenon over time, remote sensing-based change detection can be used to identify changes in the object or phenomenon's state (Nistor et al., 2021). There are many ways to examine land degradation, including Remote Sensing (RS) and field measurements (Krishan et al., 2009). In comparison to field measurements, remote sensing is much more efficient at measuring large amounts of land in a short period of time with minimal effort and at a lower cost (Vivekananda et al., 2021).

Land degradation refers to the deterioration of the quality and productivity of land, often caused by human activities and natural processes. It involves the decline in the capacity of land to support ecosystems and provide essential services, such as food production, water filtration, and habitat for biodiversity. Land degradation can have severe environmental, economic, and social impacts (Saed et al., 2022). The main factors that

contribute to land degradation are desertification, deforestation, overgrazing, urbanization and climate change.

As land degradation progresses, the visual features of this dynamism can be tracked using remote sensing analyses of changes in land cover (Mariye et al., 2022; Yiran et al., 2012). Deforestation, biodiversity loss, and other forms of land degradation are all linked to change in LU/LC (Gashaw et al., 2014). Deforestation, agricultural land conversion, and land use change are all factors that can be analyzed using land use/land cover change data (Girma et al., 2022). There is evidence that human land use from one place to another of the Simen Mountains National Park has quicker soil and vegetation degradation, according to (Ludi and Hurni, 2000). (Shareef and Hasan, 2019) have studied land degradation in Kirkuk City using Landsat images and fuzzy multi criteria.

Numerous analytical methodologies, principally multi-criteria procedures, were used to define the weights of criterion and the amounts of sub-criteria in order to analyze environmental factors independent of the level of effect of the component's complex. Saaty's analytical hierarchy process (AHP) is a common method for analyzing weight (Noori et al., 2023; Saaty, 1977). However, this procedure is unable to effectively handle the skepticism and uncertainty of the decision support discernment in order to map precise statistics (V. Y. C. Chen et al., 2011). Many authors frequently use the Analytical Network Process (ANP) to overcome the AHP's inability to handle uncertainty (Hasti et al., 2022; Moradpanah et al., 2022).

Images from various dates must be classified, and then the both classified thematic maps must be compared. As a result, the accuracy of the change map is directly related to the accuracy of the classifications itself (Lyons et al., 2018; Serra et al., 2003). In this study of land degradation, ANP was used because there is no study previously used ANP for land degradation, however, to overcome the uncertainty of AHP. Furthermore, using RS, GIS, and the multi-criteria ANP technique, this study evaluates the LULC and maps the environmental elements that affect degradation as the LULC levels developed between the period 2013 and 2021.

2. Study Area

As the seat of Nineveh Governorate, Mosul City is one of the most important cities in northern Iraq. Mosul is located around 400 kilometers (250 miles) north part of Baghdad City on the Tigris River. The old city of Mosul on the western side has expanded to include large sections on both the "Left Bank" (east side) and the "Right Bank" (west side) of the riverbanks, as residents refer to them. The ancient Assyrian city of Nineveh can be found on the east side of Mosul City. The study area has been chosen due to its rapid urban expansion and lack of vegetation during this period which caused clear land degradation. The study area is shown in Figure 1.

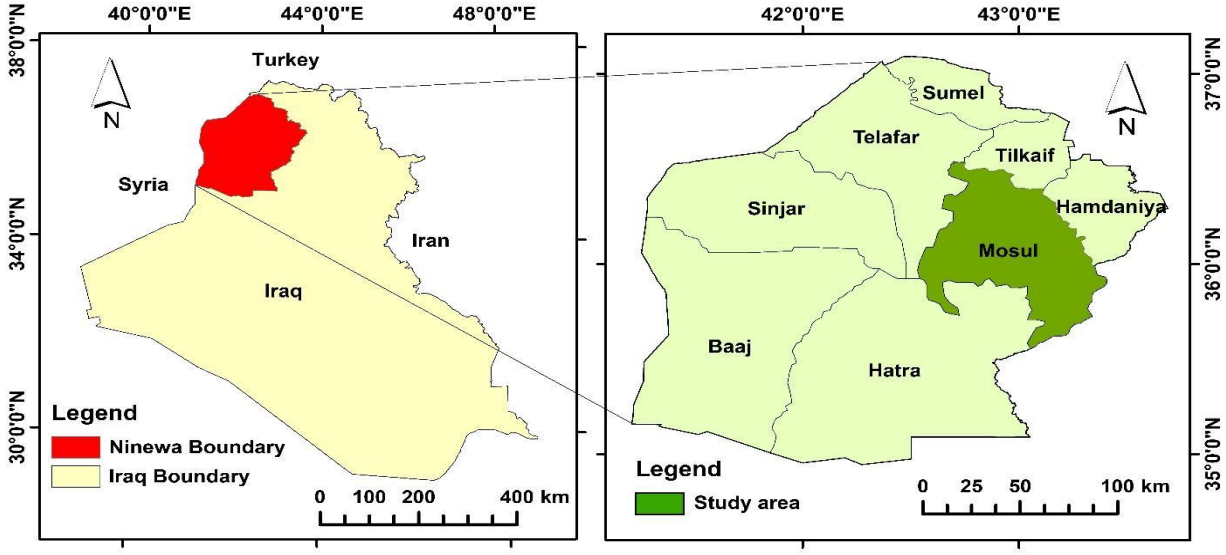

Fig.1 Study area of Mosul City

Materials and Methods

3.1 Data used and processing

This analysis relied on Landsat 8 OLI images taken in 2013 and 2021. Table 1 provides a breakdown of the satellite data. USGS Explore is used to download these 30m-resolution datasets. For this set of images, we considered the time of year and the amount of cloud cover present. Secondary data, such as administrative border shape files or information on the governorate, were employed to support the study. High-resolution satellite photos are included with the demographic and population data (RGB). The field observation is also utilized to evaluate the overall accuracy and to confirm the categorization images produced by the system.

Table 1 Details of Landsat image data acquisition

Location	Sensor	Date of Acquisition	Resolution	Cloud percentage
Mosul city data	Landsat 8	2013-07-08	30 meter	0 %
	Landsat 8	2021-07-14	30 meter	0 %

Pre-processing images is an important step in image processing since it ensures that subsequent steps will run more smoothly (Asokan and Anitha, 2019). In this study, ENVI5.3 and GIS software were used to accomplish image stacking and radiometric corrections in this research paper. All images were classified and land-use features extracted using the Maximum Likelihood classification (ML) by its role as a supervised classifier (Sisodia et al., 2014). Five feature classes were created for Landsat images; vegetation, urban, soil, bare soil, and water.

To verify the validity of the approach, high-resolution of satellite images data and field data are used. The accuracy evaluation is applied to evaluate the impotency of the algorithms that are being utilized in the project. The confusion matrix is one of the most common ways to express the precision of a precise categorization. Understanding the relationship between ground truth and classification results under inequalities in classes that are provided by this matrix. The matrix of error largely consists of the accuracy of both producers and users, and the Kappa coefficient. It's a metric for gauging how well a classification algorithm performs. The overall methodology of this study is illustrated in (Fig. 2).

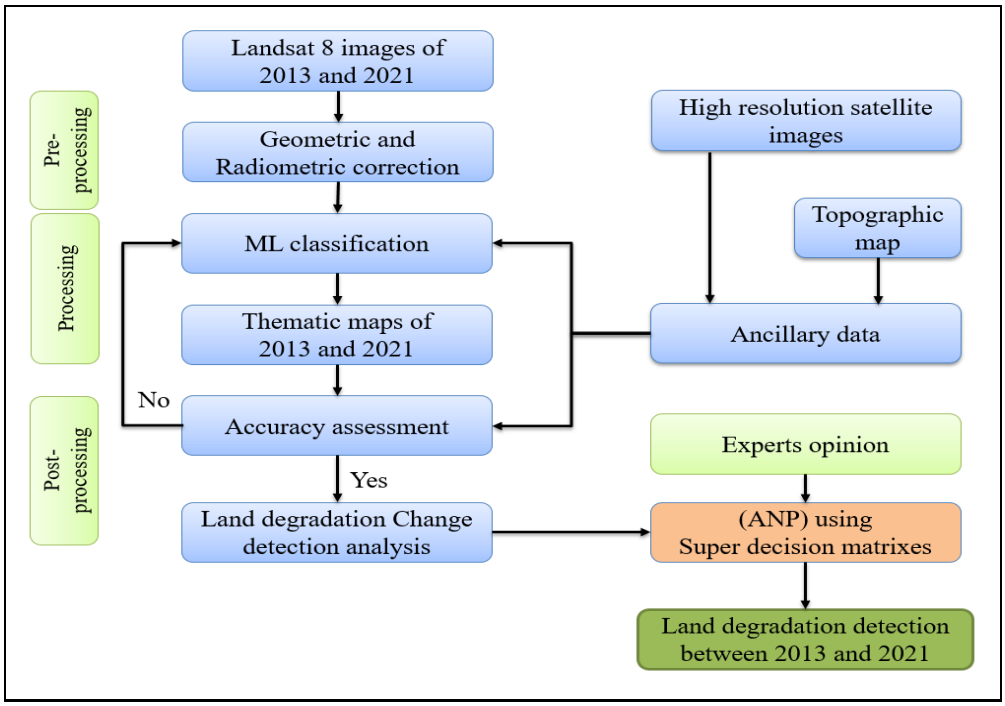

Fig. 2 Overall methodology of the study

3.2 Change Detection Process

Detecting changes in land cover using remote sensing has become an essential part of efforts to keep tabs on land degradation over the course of multiple time periods. Geometric correction and radiometric normalization were required previously by the satellite data that can be converted and classified. It is an intermediate step that enhances or produces images for classification to extract change detection information. Every step of the image enhancement process was completed using software ENVI 5.3.

The primary advantage of this method is that it provides accurate information about the transformation, which is not greatly influenced by external factors, such as atmospheric interference. LULC change detection was accomplished through the use of a post classification technique. It was used to detect the main change classes from a major pixel using a comparison-based method. A variety of techniques are used to differentiate, recognize, and define variations in data used at different times or in different situations. As a result, a classified image is generated using the change detection method's difference map to illustrate the differences between the primary image and the most recent set of data. Here, the final image was subtracted from its predecessor, and change thresholds can be applied to define the generated classes' changes. Statistical analysis was also used to compile a detailed comparison table between two classification images. There is information about image change classes, ratios, and the areas and pixel counts in the statistical record that was compiled from the data.

3.3 Analytical Network Process (ANP)

According to Saaty (1996), the super matrix technique can be used to enhance the AHP algorithm by bearing in mind a variety of decision feedback schemes that includes ANP (Eldrandaly, 2013). Since this method does not rely on classification, it can handle more difficult problems. The flexibility of this method is one of its most significant advantages. Interconnecting decision levels and decision factors at a stage that is often overlooked is an important consideration when making a decision. This technique is effective because it breaks down difficult decision-making problems (Saaty and Vargas, 2006). Many researchers are interested in the ANP's distinct advantages over the AHP. The following are the steps involved in the ANP model (Saaty, 1977):

It is important to identify and determine all of its parts, as well as their relationships to each other, in order to build a complete picture of the network. Inputting criteria and sub criteria into a matrix, comparing them side by side, and computing the consistency ratio and decision sustainability. Using the Eigenvector method to calculate the relative importance of various decision-making factors. Using the weights acquired from the Eigenvector way in the earlier stage, create a weightless super matrix from the judgmental structure. The ANP was used by the Super Decisions software to determine the final parameter weights.

$$
W=\begin{array}{c}
\\
C_1 \\
\\
\vdots \\
\\
C_K \\
\\
\vdots \\
\\
C_n \\
\\
\end{array}
\begin{array}{c}
\begin{array}{cccccc} C_1 & & \cdots & C_K & & \cdots & C_n \\ e_{11}e_{12}\cdots e_{1m1} & & \cdots & e_{k1}e_{k2}\cdots e_{km1} & & \cdots & e_{n1}e_{n2}\cdots e_{nm1} \end{array} \\
\begin{array}{c} e_{11} \\ e_{12} \\ \vdots \\ e_{1m1} \\ \vdots \\ e_{k1} \\ e_{k1} \\ \vdots \\ e_{kmk} \\ \vdots \\ e_1 \\ e_2 \\ \vdots \\ e_{nm1} \end{array}
\begin{bmatrix} W_{11} & \cdots & W_{k1} & \cdots & W_{1n} \\ \vdots & & \vdots & & \vdots \\ W_{k1} & \cdots & W_{kk} & \cdots & W_{kn} \\ \vdots & & \vdots & & \vdots \\ W_{n1} & \cdots & W_{nk} & \cdots & W_{nn} \end{bmatrix}
\end{array}
\qquad \text{eq. 1}
$$

Where, Ck is the kth cluster (k = 1, 2... N) which has nk elements denoted as ek1, ek2... eknk. A matrix segment, Wij, represents a relationship between the ith cluster and the jth cluster. Each column of Wij is a local priority vector obtained from the corresponding pairwise comparison, representing the importance of the elements in the ith cluster on an element in the jth cluster. There is no correlation between the matrix segments if there are no clusters (Lee et al., 2009).

At this point, it is possible to raise the weighted matrix to powers and transform it into the limit matrix. When the weighted super matrix is multiplied, all of the super matrix's possible paths of influence transmission are taken into account. Figure 3 demonstrate a criteria relationships based on super decision software which were applied by super matrix to produce final weights. However, the final weights have produced from the super decision software which has been illustrated in Table 2.

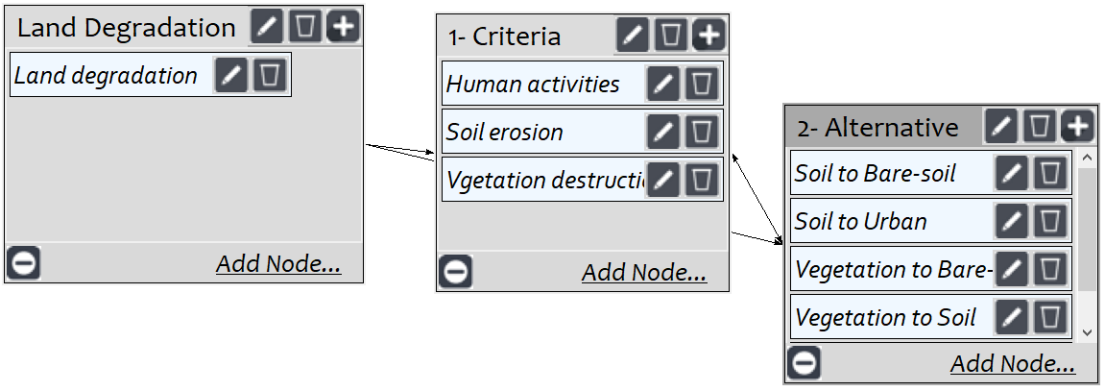

Fig. 3 Criteria relationships based on super decision software

Table 2 Final weights of land degraded criteria

Criteria	Weight
Vegetation to Urban	0.564
Vegetation to Bare soil	0.245
Vegetation to Soil	0.135
Soil to Urban	0.037
Soil to Bare soil	0.017

Result And Discussion

4.1 Classification Results

Figure 4 depicts the spatial distribution for five types of land cover for 2013, whereas Figure 6 shows the percentage of each type and its corresponding area, both in percentage and in square meters. Soil accounts for 32.57 percent of the study area, or 299.65 km^2, and is the most common class. In contrast, only 12.93 percent of the total study area is occupied by the urban category, with a total area of 119.04 km^2. Approximately 30.67 percent of the study area, or 282.23 km^2, is covered by bare soils which are the second highest percentage. At 22.64 percent or 208.28 km^2, vegetation makes up the third-largest portion of the area of research. However, water covering 1.19% of the study area or 10.95 km^2.

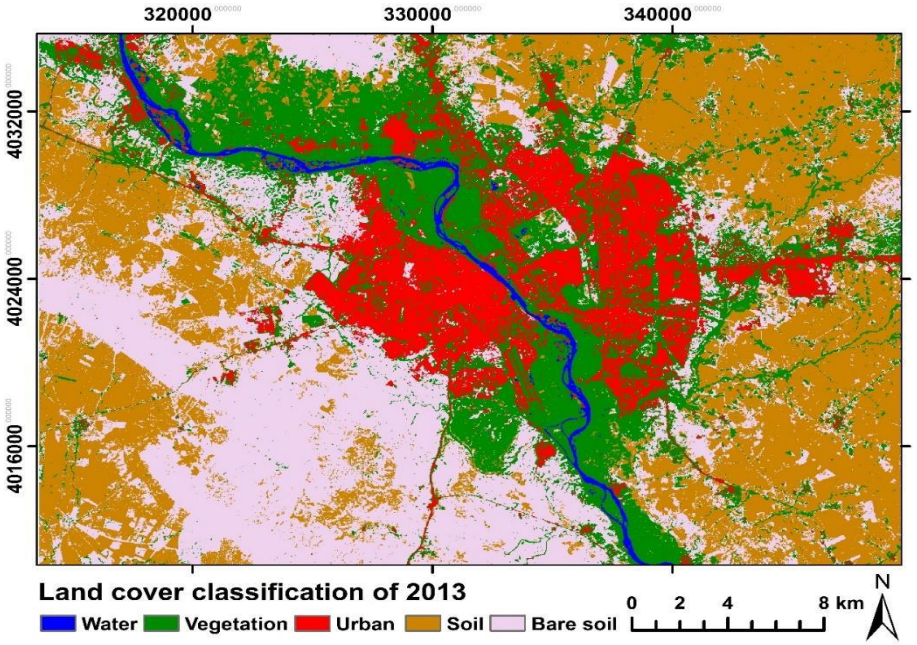

Fig. 4 Land cover classification of 2013 using ML classification.

Figure 5 depicts the spatial distribution of five types for land cover for 2021, while Figure 6 shows the percentage of each type and its corresponding area. The majority of the study area, or 476.19 km^2, is comprised of bare soil, which interpretates for 51.75% of the total area. However, the vegetation class covers only 61.23 km^2 of the study area, which is only 6.66 percent of the total area. The urban portion of the study area makes up the second-highest percentage, at approximately 21.82% or 200.76 square kilometers. Approximately 18.81 percent of the study area, or 173.12 km^2, is made up of soil. However, water covering 0.96% of the study area or 8.86 km^2.

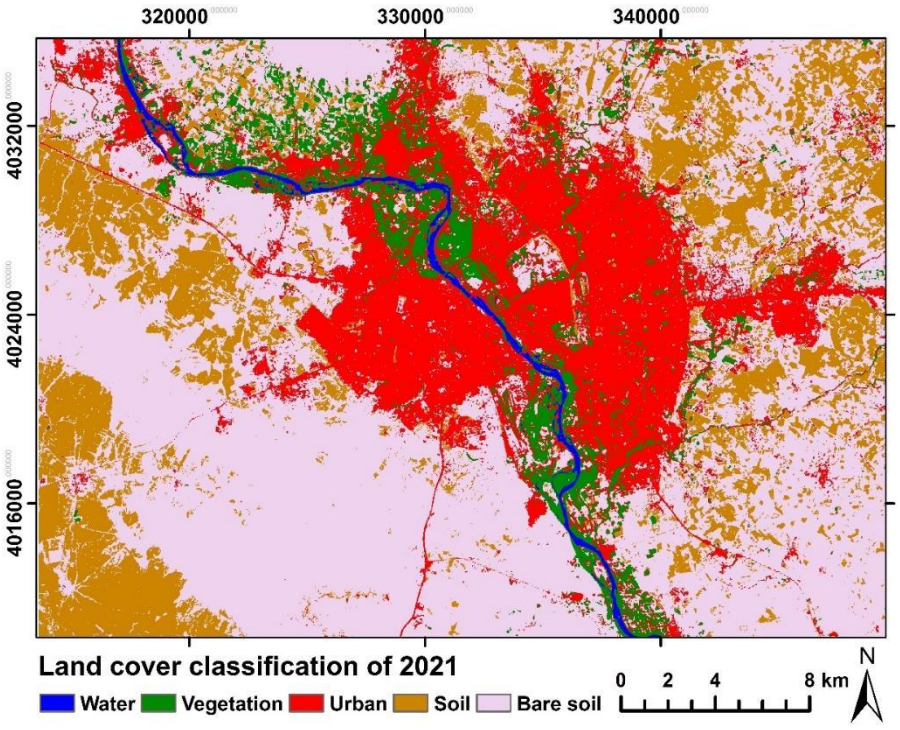

Fig. 5 Land cover classification of 2021 using ML classification

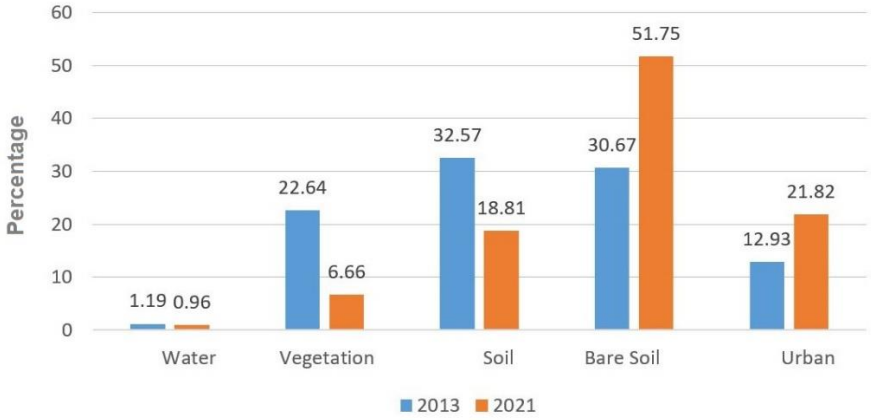

Fig.6 Land cover classes percentages for 2013 and 2021

4.2 Accuracy assessment

Each year's ML classifier results are shown in Table 3 using confusion matrices to evaluate classification efficiency. The percentage of pixels that are correctly classified is what we mean by "overall accuracy". For different time periods between 2013 and 2021, the classifier's overall efficiencies ranged from 98.62 percent and 98.06 percent respectively, based on Kappa coefficients of 0.9649 and 0.984. Users' accuracy (UA) and producers' accuracy (PA) are both defined by how likely it is that an image pixel in the classified image matches an image pixel in the ground truth data.

Table 3 Components of the data used to create the confusion matrix

Class	2013		2021	
	Prod. Acc. (Percent)	User Acc. (Percent)	Prod. Acc. (Percent)	User Acc. (Percent)
Water	95.44	100.00	99.52	100.00
Vegetation	100.00	81.94	100.00	95.09
Urban	99.53	100.00	99.91	98.72
Soil	89.40	98.98	93.63	98.11
Bare Soil	99.69	97.24	99.53	99.38
Overall accuracy	97.55%		98.91%	
Kappa confidence	0.9627		0.9840	

4.3 Change detection analysis

Figure 7 and the data in Tables 4 and 5 were used to determine and analyze the shifts that occurred between the period 2013 and 2021. In addition, the analysis resulted in the identification of the factors that influenced the changes. There was a dramatic decrease in vegetation from 22.67% to 6.666%, mainly due to the climate effect of rainfall precipitation. However, vegetation changes to urban according to rapid urban growth. During this time period, the urban class increased significantly, with net change percentages ranging from 12.93% to 21.82 %, as a result of increasing population growth, particularly in the study area's major cities.

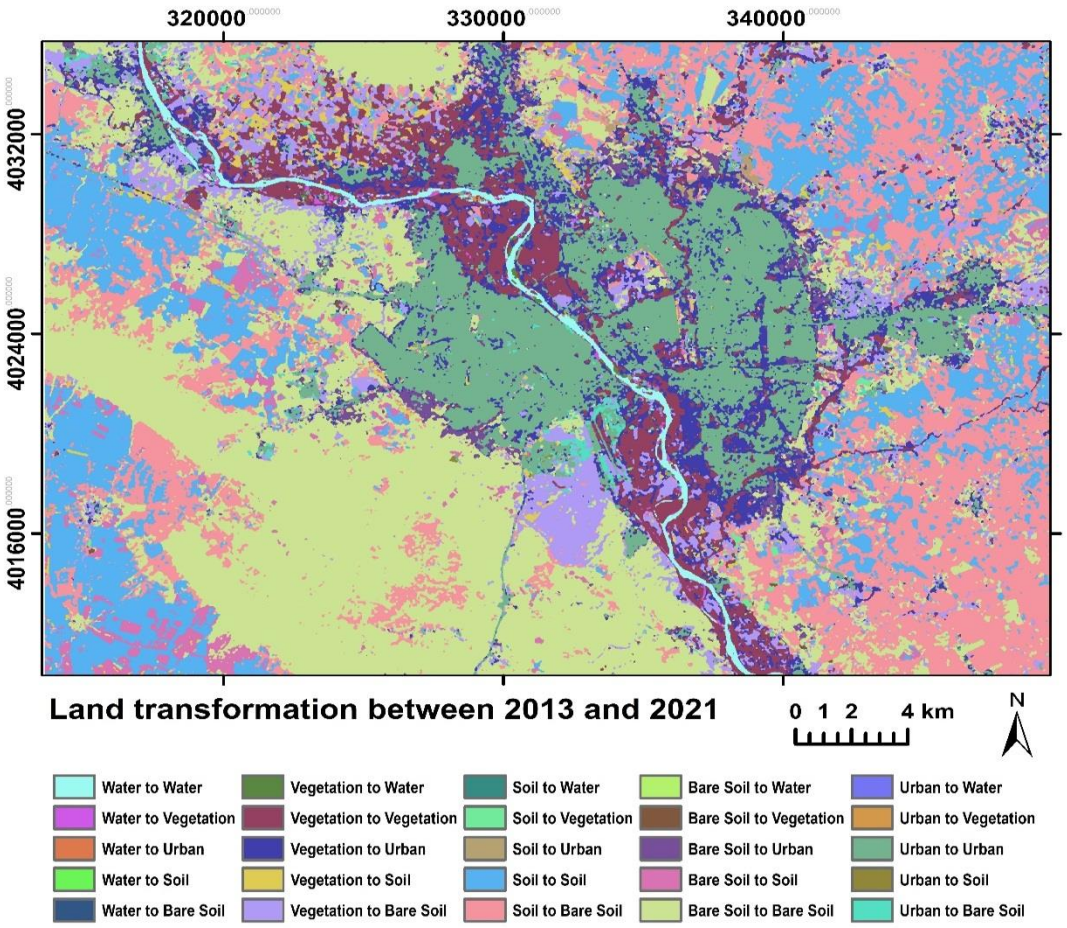

Fig. 7 Change detection map between the period 2013 and 2021

Table 4 Percentages change of land cover classes between the period 2013 and 2021

Classes	Water	Vegetation	Urban	Soil	Bare Soil	Class Total
Water	72.220	0.406	0.073	0.004	0.004	100
Vegetation	22.306	25.691	0.689	0.962	0.556	100
Urban	4.668	33.151	93.138	1.615	5.487	100
Soil	0.074	7.961	0.520	42.184	10.454	100
Bare Soil	0.731	32.791	5.580	55.235	83.499	100
Class Total	100	100	100	100	100	-
Class Changes	27.780	74.309	6.862	57.816	16.501	-

Table 5 Area (m^2) change of land cover classes between the period 2013 and 2021

Classes	Water	Veget.	Urban	Soil	Bare Soil	Class Total
Water	7908300	845100	87300	11700	9900	8862300
Veget.	2442600	53511300	819900	2883600	1568700	61226100
Urban	511200	69048900	110875500	4839300	15486300	200761200
Soil	8100	16580700	619200	126403200	29505600	173116800
Bare Soil	80100	68298300	6642900	165512700	235659600	476193600
Class Total	10950300	208284300	119044800	299650500	28220100	-
Class Change	3042000	154773000	8169300	173247300	46570500	-

4.4 Land degradation

ANP analysis and change detection criteria were used to create the final map of Mosul's degeneration. A degradation index based on these criteria has been in use over time. In the index, the factors that have a negative impact on land quality are listed. Degradation Index can thus be illustrated as follows:

DI = 0.564×VU + 0.245×VB + 0.135×VS + 0.037 SU + 0.017× SB *(eq. 2*)

DI is the degradation index. However, VU denotes to the changing the vegetation to urban. While, VB is the translating of vegetation to bare soils, VS is the altering of vegetation to soil. Furthermore, SB refers to the transforming the Soil to bare soil and SU denotes to the changing of soil to urban (Table 6). The map of land degradation from the period 2013 to 2021 was generated using the producing index as shown in equation 2. Figure 8 illustrate Land degradation monitoring potential map of Mosul City.

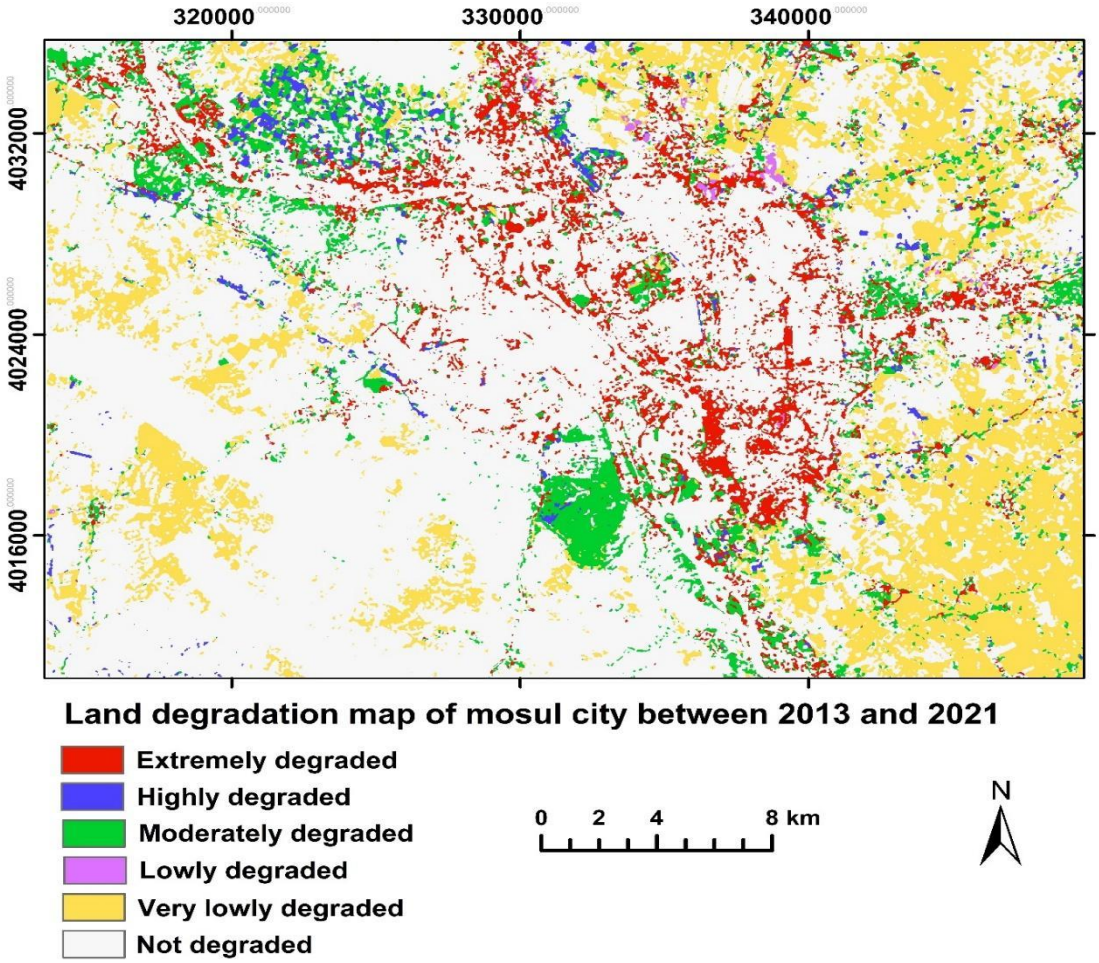

Fig. 8 Land degradation monitoring potential map of Mosul City

Table 6 Land degradation between the period 2013 and 2021

Classes change	Land degradation	Area (km^2)
Vegetation to Urban	Extremely degraded	64.546200
Vegetation to Bare soil	Highly degraded	13.611600
Vegetation to Soil	Moderate degraded	64.580400
Soil to Urban	Lowly degraded	3.038400
Soil to Bare soil	Very lowly degraded	167.342400

Addressing land degradation requires a combination of sustainable land management practices, policy interventions, and community engagement. These may include measures such as implementing soil conservation techniques, promoting sustainable agriculture, reforestation and afforestation, restoring degraded lands, and implementing land-use planning strategies that prioritize conservation and sustainable development.

Conclusion

Changing LULC evaluations and their importance to support mapping and decision making is one of the greatest significant aspects of the study areas' urbanization. This study used ENVI, ANP, and GIS to examine Landsat temporal data between the period 2013 and 2021. Between 2013 and 2021, there was a steady increase in urban and water classes, as well as a decrease in vegetation. Mosul's map degradation's suitability was assessed using an algorithm developed with the ANP. It was determined that the vegetation and soil feature classes were the most important factors in determining the extent of degradation, compared to other factors, such as urban and bare soil. Vegetation is being reduced in the study area, the conversion of soil to urban or bare soil have resulted in a wide range of environmental degradation. According to the map of degradation, the most degraded areas are classes that have been transformed from vegetation class to urban and bare soil classes, as well as those that have been converted from soil class to urban and bare soil classes. GIS and ANP methods proved to be an effective strategy for assessing land degradation, according to the results of this study.

References

[1] Asokan, A., and Anitha, J. (2019). Change detection techniques for remote sensing applications: a survey. Earth Science Informatics, 12(2), 143–160.

[2] Chen, S., and Rao, P. (2008). Land degradation monitoring using multi-temporal Landsat TM/ETM data in a transition zone between grassland and cropland of northeast China. International Journal of Remote Sensing, 29(7), 2055–2073.

[3] Chen, V. Y. C., Lien, H.-P., Liu, C.-H., Liou, J. J. H., Tzeng, G.-H., and Yang, L.-S. (2011). Fuzzy MCDM approach for selecting the best environment-watershed plan. Applied Soft Computing, 11(1), 265–275.

[4] Collado, A. D., Chuvieco, E., and Camarasa, A. (2002). Satellite remote sensing analysis to monitor desertification processes in the crop-rangeland boundary of Argentina. Journal of Arid Environments, 52(1), 121–133.

[5] Eldrandaly, K. A. (2013). Exploring multi-criteria decision strategies in GIS with linguistic quantifiers: an extension of the analytical network process using ordered weighted averaging operators. International Journal of Geographical Information Science, 27(12), 2455–2482.

[6] Gashaw, T., Bantider, A., and Mahari, A. (2014). Evaluations of land use/land cover changes and land degradation in Dera District, Ethiopia: GIS and remote sensing based analysis. International Journal of Scientific Research in Environmental Sciences, 2(6), 199.

[7] Geerken, R., and Ilaiwi, M. (2004). Assessment of rangeland degradation and development of a strategy for rehabilitation. Remote Sensing of Environment, 90(4), 490–504.

[8] Girma, R., Fürst, C., and Moges, A. (2022). Land use land cover change modeling by integrating artificial neural network with cellular Automata-Markov chain model in Gidabo river basin, main Ethiopian rift. Environmental Challenges, 6, 100419.

[9] Hasti, F., Rouhi, H., Pezhooli, N., SalmanMahiny, A., and Rostami, H. (2022). Zoning and spatial vulnerability assessment with emphasis on infrastructure using GIS (case study: Kurdistan Province, Iran). Arabian Journal of Geosciences, 15(1), 1–17.

[10] Jayanth, J., Aravind, R., and Amulya, C. M. (2022). Classification of crops and crop rotation using remote sensing and GIS-based approach: A case study of Doddakawalande Hobli, Nanjangudu Taluk. Journal of the Indian Society of Remote Sensing, 50(2), 197–215.

[11] Krishan, G., Kushwaha, S. P. S., and Velmurugan, A. (2009). Land degradation

mapping in the upper catchment of river Tons. Journal of the Indian Society of Remote Sensing, 37(1), 119–128.

[12] Lee, H., Kim, C., Cho, H., and Park, Y. (2009). An ANP-based technology network for identification of core technologies: A case of telecommunication technologies. Expert Systems with Applications, 36(1), 894–908.

[13] Ludi, E., and Hurni, H. (2000). Reconciling conservation with sustainable development: A participatory study inside and around the Simen Mountains National Park, Ethiopia. Centre for Development and Environment.

[14] Lyons, M. B., Keith, D. A., Phinn, S. R., Mason, T. J., and Elith, J. (2018). A comparison of resampling methods for remote sensing classification and accuracy assessment. Remote Sensing of Environment, 208, 145–153.

[15] Mariye, M., Maryo, M., and Li, J. (2022). The study of land use and land cover (LULC) dynamics and the perception of local people in Aykoleba, northern Ethiopia. Journal of the Indian Society of Remote Sensing, 50(5), 775–789.

[16] Moradpanah, M., Monavari, S. M., Shariat, S. M., Khan Mohammadi, M., and Ghajar, I. (2022). Evaluation of Ecological Vulnerability of Coasts of the Caspian Sea Based on Multi-criteria Decision Methods (Iran). Journal of the Indian Society of Remote Sensing, 50(12), 2479–2502.

[17] Nistor, C., Vîrghileanu, M., Cârlan, I., Mihai, B.-A., Toma, L., and Olariu, B. (2021). Remote Sensing-Based Analysis of Urban Landscape Change in the City of Bucharest, Romania. Remote Sensing, 13(12), 2323.

[18] Noori, S., Ghasemlounia, R., and Noori, A. M. (2023). Site Suitability in Water Harvesting Management Using Remote Sensing Data and GIS Techniques: A Case Study of Sulaymaniyah Province, Iraq. In Climate Change, Agriculture and Society: Approaches Toward Sustainability (pp. 227–257). Springer.

[19] Saaty, T. L. (1977). A scaling method for priorities in hierarchical structures. Journal of Mathematical Psychology, 15(3), 234–281.

[20] Saaty, T. L., and Vargas, L. G. (2006). Decision making with the analytic network process (Vol. 282). Springer.

[21] Saed, F. G., Noori, A. M., Kalantar, B., Qader, W. M., and Ueda, N. (2022). Earthquake-Induced Ground Deformation Assessment via Sentinel-1 Radar Aided at Darbandikhan Town. Journal of Sensors, 2022.

[22] Serra, P., Pons, X., and Sauri, D. (2003). Post-classification change detection with data from different sensors: some accuracy considerations. International Journal of Remote Sensing, 24(16), 3311–3340.

[23] Shareef, H., and Hasan, N. (2019). Integrating of GIS and fuzzy multi-criteria method to evaluate land degradation and their impact on the urban growth of Kirkuk city, Iraq. International Journal of Advanced Science and Technology, 28(15), 800–815.

[24] Sisodia, P. S., Tiwari, V., and Kumar, A. (2014). Analysis of supervised maximum likelihood classification for remote sensing image. International Conference on Recent Advances and Innovations in Engineering (ICRAIE-2014), 1–4.

[25] Vivekananda, G. N., Swathi, R., and Sujith, A. (2021). Multi-temporal image analysis for LULC classification and change detection. European Journal of Remote Sensing, 54(sup2), 189–199.

[26] Yiran, G. A. B., Kusimi, J. M., and Kufogbe, S. K. (2012). A synthesis of remote sensing and local knowledge approaches in land degradation assessment in the Bawku East District, Ghana. International Journal of Applied Earth Observation and Geoinformation, 14(1), 204–213.